scientific reports



OPEN

Cerumenogram as an assay for the metabolic diagnosis of precancer, cancer, and cancer remission

João Marcos Gonçalves Barbosa¹, Camilla Gabriela de Oliveira¹,
Marina Ferraz Gontijo Soares¹, Larissa Fernanda Medeiros Vieira², Omar Carneiro Filho²,
Daniela Medeiros Milhomem Cardoso³, Patricia Medeiros Milhomem Beato⁴,
Cristina Aparecida Trigo Martins Moro⁴, Anselmo Elcana de Oliveira⁵ &
Nelson Roberto Antoniosi Filho^{1⊠}

Early diagnosis is crucial for successful cancer treatment. As a mitochondrial metabolic disease, cancer produces volatile organic metabolites that are present in earwax, allowing differentiation between healthy individuals and those with cancer through an assay called cerumenogram. In this case series study, we demonstrated that this assay also enables the diagnosis of precancerous stages, such as hypermetabolic inflammation and dysplasia, which can aid in treatments to prevent cancer progression. Additionally, this assay reveals that oncological metabolism differs from that observed in metaplasias, cysts, and benign tumors, helping to avoid unnecessary oncological procedures due to suspected malignancy. Cerumenogram can also be used to assess cancer remission. Thus, the cerumenogram emerges as an assay that might enable the diagnosis of cancer, monitor remission, and identify precancerous stages, covering key steps of tumorigenesis.

Keywords Volatile organic compounds, Carcinogenesis, Early diagnosis, Biomarkers, Earwax, Cerumenogram

Galen's (129–199 AD) statement that tumors could be cured through cauterization in their early manifestation stages was probably the first to underline the importance of early cancer diagnosis for better treatment outcomes¹. Current cancer data support this observation, first made in ancient Greece, showing that early tumor diagnosis can substantially increase a patient's five-year survival rate by more than 90% for almost all cancer types², leading to a greater chance of complete cancer remission by treatment. However, approximately 90% of all cancers are detected symptomatically when half of the cases are at an advanced stage³, representing approximately 70% of deaths due to late diagnosis in low- and middle-income countries^{4,5}.

Early cancer detection relies on a fundamental understanding of one of the hallmarks of cancer, the dysregulation of cellular metabolism⁶, which drives abnormal growth and differentiation in cells⁷. The energetic rewiring of differentiated cells is linked to mitochondrial dysfunction⁸, which may pave the way for transforming cells from a healthy to a malignant state by inducing metabolic disorders and epigenetic alterations that drive them to evade apoptosis. Early detection involves monitoring the metabolic changes induced by mitochondria-associated tumor precursors that trigger the transition from regular cellular activity until the beginning of cancer cell formation³.

Omics research has shed light on the mechanisms that drive cell transformation from a regular to a precancerous state⁷. Recent studies have demonstrated that specific genes are crucial for transforming precancerous lesions into cancerous lesions; for example, TP53 biallelic loss promotes early carcinogenesis in esophageal squamous cell carcinoma, inducing normal tissue transformation into early precancerous lesions⁹. An equal effect was observed for oral precancerous lesions in which TP53 mutations were shared between dysplasia and carcinoma¹⁰.

¹Laboratório de Métodos de Extração e Separação (LAMES), Instituto de Química (IQ), Universidade Federal de Goiás (UFG), Campus II – Samambaia, Goiânia, GO 74690-900, Brazil. ²Insituto de Medicina Nuclear (IMEN), Alameda dos Buritis, 600, St. Central, Goiânia, GO 74015-080, Brazil. ³Instituto do Aparelho Digestivo (IAD), R. 34, 157, St. Marista, Goiânia, GO 74150-220, Brazil. ⁴Hospital Amaral Carvalho (HAC), R. Dona Silvéria, 150, Chácara Braz Miraglia, Jaú, SP 17210-070, Brazil. ⁵Laboratório de Química Teórica e Computacional (LQTC), Instituto de Química (IQ), Universidade Federal de Goiás (UFG), Campus II – Samambaia, Goiânia, GO 74690-970, Brazil. ™email: nelsonroberto@ufg.br

Another metabolic signature in premalignant cells is genome instability induced by reactive oxygen species (ROS), which leads to mitochondrial dysfunction in the early stages of abnormal cell proliferation¹¹. Mitochondrial dysfunction due to energy rewiring, a consequence of mitochondrial DNA instability, seems to be a pivotal driver of cell transformation from a healthy to a malignant state¹². Mitochondrial oxidative stress due to increased ROS levels in malignant cells leads to cell membrane damage, inducing the breakdown of organelles, mitochondrial cristae, lipids, carbohydrates, and proteins and the release of small metabolites in the bloodstream, also known as volatile organic metabolites (VOMs)^{13,14}.

Recently, cerumen (earwax) has been identified as an exciting source of ROS-derived mitochondrial volatile metabolites for the study of metabolic disturbances in the human body, mainly because of its ability to concentrate polar and nonpolar compounds excreted by sebaceous and sweat glands¹⁵. In recent years, we have explored headspace/gas chromatography-mass spectrometry (HS/GC-MS) assays using earwax as a biofluid for veterinary investigations, such as tracking metabolic changes occurring during the transition period between late pregnancy and early lactation¹⁶, trypanosomiasis¹⁷, lameness¹⁸, biomarkers for hepatotoxicity associated with toxic plant ingestion¹⁹, and environmental exposures^{20,21}. We also employed this assay to identify diabetes mellitus and xenobiotic exposures^{22,23}. In recent studies, we have demonstrated that cerumen metabolites can discriminate between cancer and control (cancer-free) cohorts in humans²⁴ and dogs²⁵. The panel of candidate biomarkers identified for humans and dogs comprised metabolites that may be mainly linked to lipid metabolism and oxidative stress associated with mitochondrial dysfunction^{24,25}, a fingerprint of metabolic rewiring in malignant cell proliferation for several types of cancer²⁶.

The assay for cancer discrimination using earwax is called "Cerumenogram"²⁴. It comprises a bioanalytical protocol with a noninvasive and low-risk sample collection procedure, minimal sample preparation, and sensitive and robust analysis of VOMs via headspace/gas chromatography-mass spectrometry (HS/GC-MS), followed by machine learning algorithms for the monitoring and detection of discriminant metabolites. In this approach, the results of a test sample classification can be visualized by their similarity with the cancer or non-cancer group in a circular or linear dendrogram, *i.e.*, the test sample clustered among the cancer (oncological risk) or non-cancer (oncological risk-free) samples (Figure S1). Thus, while some oncological examinations, such as positron emission tomography with 2-deoxy-2-[fluorine-18]fluoro-D-glucose integrated with computed tomography (¹⁸F-FDG PET/CT), are based on glycolytic metabolism, the cerumenogram assay relies on biomarkers derived from glycolytic and mainly by lipid metabolism (such as hydrocarbons, ketones, aldehydes, organic acids, and furans) to discriminate between volunteers with and without cancer.

Given the importance of early cancer detection-including monitoring premalignant cells, addressing mitochondrial dysfunctions associated with cell transformation, and exploring the potential of earwax as a source of essential ROS-derived mitochondrial volatile metabolites—a new opportunity has emerged: utilizing the cerumenogram as a practical diagnostic tool to identify oncological risks in premalignant lesions before cancer develops, as well as to differentiate metaplasia and benign tumors from other stages of tumorigenesis. This study discusses several innovative cases of applying the cerumenogram to detect precancerous and early malignant manifestations while demonstrating its effectiveness as a follow-up tool for monitoring cancer remission.

Results

Cerumenogram model

A Cerumenogram-based model was used to classify the samples as part of the "oncological risk" or "oncological risk-free" groups. The cerumenogram-based model was developed using biomarkers with a higher frequency of occurrence in the cancer cohort²⁴. A receiver operating characteristic (ROC) curve-based evaluation model was built by selecting a logistic regression algorithm method classification for binary variables²⁷. The logistic regression model performance was calculated using tenfold cross-validation (CV), reaching an area under a curve (AUC), sensitivity, and specificity of 0.916 (0.858–0.974), 0.904 (0.904–0.984), and 0.880 (0.790–0.970), respectively, after CV.

All cerumen samples collected from 531 volunteers with cancer (Table 1) were analyzed by HS/GC-MS and assessed using a cerumenogram assay to verify the presence of cancer in the volunteers. Some examples of these results for each type of cancer at different stages are shown in Supplementary Figures \$2-\$10. These findings confirmed the suitability of cerumenogram for diagnosing cancer at different stages. In the self-declared control group (n = 203), 200 samples were classified as negative by the cerumenogram assay; however, three samples were classified as positive by the cerumenogram assay, and the volunteers agreed to undergo further evaluation to investigate these results. Further clinical evaluation confirmed hypermetabolic inflammation in two volunteers (see sections Hypermetabolic Inflammation in the Ascending Colon and Hypermetabolic Inflammation in the Zygomaticus Minor and Major Muscle) and cancer recurrence in one patient (see the section Detection of Cancer Recurrence Until Remission Using the Cerumenogram).

Hypermetabolic inflammation in the ascending colon

The volunteer was a 44-year-old white Brazilian male with a body mass index of 25 kg m⁻² and no previous medical history of oncological disease. In the first sample collection, during a round of sample collection for Phase II (which involved increasing the sample size) of the Cerumen Project, the volunteer was assigned to the control group (oncological risk-free). However, even though the volunteer self-identified as part of the control group, the cerumenogram analysis indicated that the sample was part of the case group (oncological risk). Table 2 summarizes the sample collection number, event and date, cerumenogram results, and the actions at each study step. The volunteer agreed to conduct a follow-up to investigate whether the result was a false positive in the cerumenogram model or indicated an unknown oncological manifestation (Table 2). Subsequently, a second cerumen sample was collected from the volunteer for analysis, and again, the test showed that the volunteer

Local of primary cancer	Number of samples	Stage groups (I-IV)
Colorectal, prostate, and bladder	210	I-IV
Breast	73	I-IV
Hematological	42	NI
Skin	40	I-IV
Head and Neck	37	II-IV
Ovarian, uterine, and cervical	36	I-IV
Stomach, esophagus and pancreas	30	I-IV
Lung	17	III-IV
Liver	14	I–III
Kidney	12	I, III–IV
Testicular	6	I–II, IV
Soft tissue	5	NI
Not Informed (NI)	9	-

Table 1. The primary cancer location and staging range of the 531 volunteers with cancer included in Phase II of the Cerumen Project (sample size increase).

Sample collection number	Event (date)	Predicted group	Actions
I	First Cerumen Analysis (Patient Self-declared as Part of the Oncological Risk-free group) (October 25, 2019)	Oncological Risk	Proof Analysis Required
II	Second Cerumen Analysis (Proof) (November 20, 2019)	Oncological Risk	Investigation of Biological Bias (Hypothesis of a Potential Biological Bias due to the Chronic Sinusitis Condition of the Volunteer
III	Cerumen Analysis After Treatment for Chronic Sinusitis (December 12, 2019)	Oncological Risk	Investigation of Chronic Sinusitis influence on the Results (Hypothesis testing)
IV	Fourth Cerumen Analysis for Patient Follow-up (February 06, 2020)	Oncological Risk	Volunteer Follow-up
V	Cerumen Analysis During the Preoperative Procedures (June 03, 2020)	Oncological Risk	Cerumenogram Test Before the Operative Procedures
VI	Cerumen, Tissue, and Sphenoid Sinuses Secretion Analysis (Surgery Day) (August 31, 2020)	Oncological Risk	Cerumenogram Test at the Endoscopic Sinus Surgery Day
VII	Last Cerumen Analysis of the Volunteer before the $^{18}\mbox{F-FDG}$ PET/CT examination (December 03, 2020)	Oncological Risk	Follow-up after the surgical procedure and imaging diagnostic indication

Table 2. Longitudinal analysis results for the Cerumenogram investigation of a volunteer self-declared as part of the oncological risk-free group but classified as part of the oncological risk group.

was part of the oncological risk group (Table 2). At this time, the volunteer reported using daily medication to treat chronic rhinosinusitis. Therefore, we collected new samples to determine if the treatment influenced the cerumenogram results.

The results confirmed that the volunteer was consistently classified in the oncological group (Table 2). Even after completing drug treatment for chronic rhinosinusitis, the volunteer reported experiencing the following symptoms: nasal inflammation, postnasal drainage, tenderness, swelling around the eyes, pain in the upper jaw and teeth, sore throat, bad breath, and fatigue. Based on the clinical findings and symptoms reported by the volunteer, the otolaryngologist recommended functional endoscopic sinus surgery.

Earwax, tissue, and sphenoid sinus secretions were collected from the volunteer on the day of surgery. Microbiological analysis of sphenoid sinus secretions revealed *Pseudomonas aeruginosa* (*P. aeruginosa*), confirming that rhinosinusitis was a bacterial infection. Interestingly, HS/GC-MS analysis of tissue and sphenoid sinus secretions revealed volatile sulfur metabolites, such as dimethyl disulfide and trisulfide (Figure S11), which are common *P. aeruginosa* metabolites biosynthesized by the derivation of methanethiol²⁸. However, after the patient reported no symptoms of sinusitis and the subsequent cerumen analyses continuously indicated a positive oncological risk (Table 2), we ruled out the hypothesis that sinus inflammation induces a false-positive result in the cerumenogram assay.

To confirm the oncological risk indicated by the cerumenogram test, the patient consented to undergo $^{18}\text{F-FDG PET/CT}$ examination. This examination is the gold standard imaging modality for assisting in diagnosis because of its ability to measure the "metabolic signature" of cells, which is strongly associated with the glycolytic metabolism of abnormal cells 29 . In the initial cell differentiation process, some mutations impair mitochondrial energy metabolism, which simulates the Warburg effect and provides a signal for $^{18}\text{F-FDG PET/CT}^{30}$.

For the volunteer under observation, ¹⁸F-FDG PET/CT examination revealed a hypermetabolic focus in the proximal third of the ascending colon, which persisted in the delayed images (Fig. 1). ¹⁸F-FDG PET/CT showed maximum standardized uptake values (SUVmax) of 8.9 g mL⁻¹ and 11.0 g mL⁻¹ in the early and delayed images, respectively. The imaging results suggested a correlation with chromoscopic colonoscopy to confirm the nature

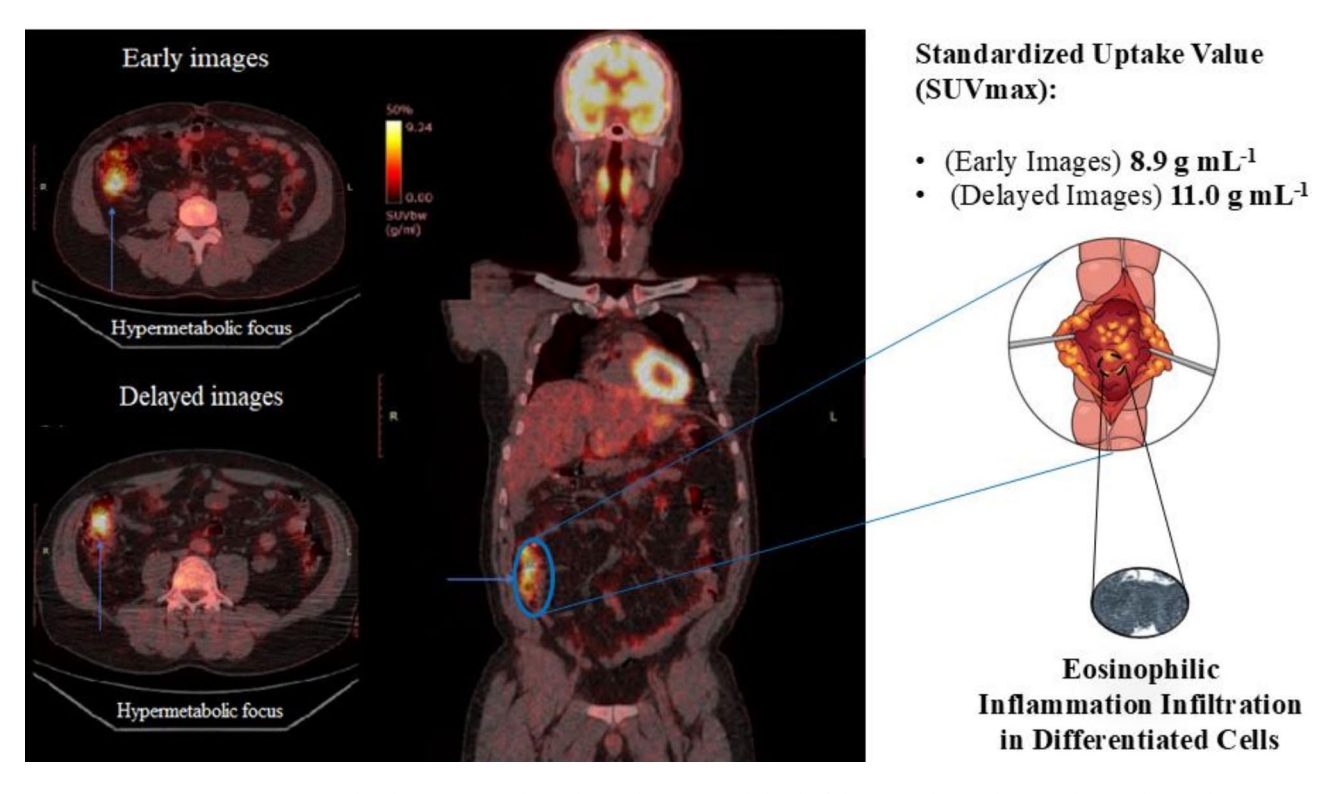


Fig. 1. Radiopharmaceutical uptake in the proximal third of the ascending colon, as observed in early images and persisting in delayed images (SUVmax: 8.9 and $11.0~{\rm g~mL^{-1}}$), with colonic biopsy revealing eosinophilic inflammatory infiltration in differentiated cells.

of the hypermetabolic manifestations. Colonic biopsy findings showed eosinophilic inflammatory infiltration in the differentiated cells (Figure S12). Previous studies have shown that tumor-associated eosinophilia is commonly observed in human cancer development, suggesting that eosinophils are part of an early inflammatory reaction at the site of tumorigenesis 31 .

In summary, the cerumenogram successfully indicated the presence of a hypermetabolic inflammatory manifestation associated with an increased risk of developing neoplasia. Thus, in this clinical case, the cerumenogram appeared to be a powerful tool for tracking potential colon cancer risk, as evidenced by the detection of a hypermetabolic lesion in the ascending colon in an asymptomatic volunteer, which was later confirmed by ¹⁸F-FDG PET/CT, chromoscopic colonoscopy, and local biopsy.

Hypermetabolic inflammation in the zygomaticus minor and major muscle

In this investigation, the volunteer was a 60-year-old Brazilian white female with a body mass index of 22 kg m⁻². Clinical anamnesis revealed hypothyroidism, gastroesophageal reflux disease, hypertension, and removal of a benign mammary nodule ten years before the date of earwax sample collection. The patient had no history of oncological diseases among her first-degree relatives.

During a round of sample collection for Phase II of the Cerumen Project, the patient was also assigned to the control group (oncological risk-free). Nevertheless, the Cerumenogram assay indicated that the volunteers were part of the case group (oncological risk). To investigate the outcome, the volunteers agreed to undergo follow-up with $^{18}\text{F-FDG}$ PET/CT. Imaging revealed a hypermetabolic region in the zygomaticus muscles with an SUVmax of 6.5 g mL $^{-1}$, probably related to high inflammatory activity, although the patient was asymptomatic. Figure 2 summarizes the results of the cerumenogram assay and $^{18}\text{F-FDG}$ PET/CT workflow applied to the patient.

Although tumor cell proliferation linked to the zygomatic muscle is uncommon³², the inflammation detected in the patient via ¹⁸F-FDG PET/CT analysis was consistent with the positive cerumenogram results for hypermetabolic inflammation. As a counterattack to the cell inflammatory response, ROS levels increase within the cell, driving genome instability and mitochondrial dysfunctions that can function as tumor-promoting processes³³.

Thus, volatile metabolites are valuable biochemical fingerprints for detecting several inflammation-induced diseases^{34,35}. As inflammation is a critical component of initial tumor progression, and volatile metabolites are associated with an endogenous inflammatory response, the possibility of using a volatilomic-based method, such as the cerumenogram, for early oncological risk is of clinical interest. In summary, the cerumenogram successfully indicated the presence of an inflammatory manifestation, as evidenced by the detection of a hypermetabolic region in the zygomaticus minor and major muscles, revealing the exciting application of this method for detecting cell conditions similar to the tumor-promoting inflammatory processes.

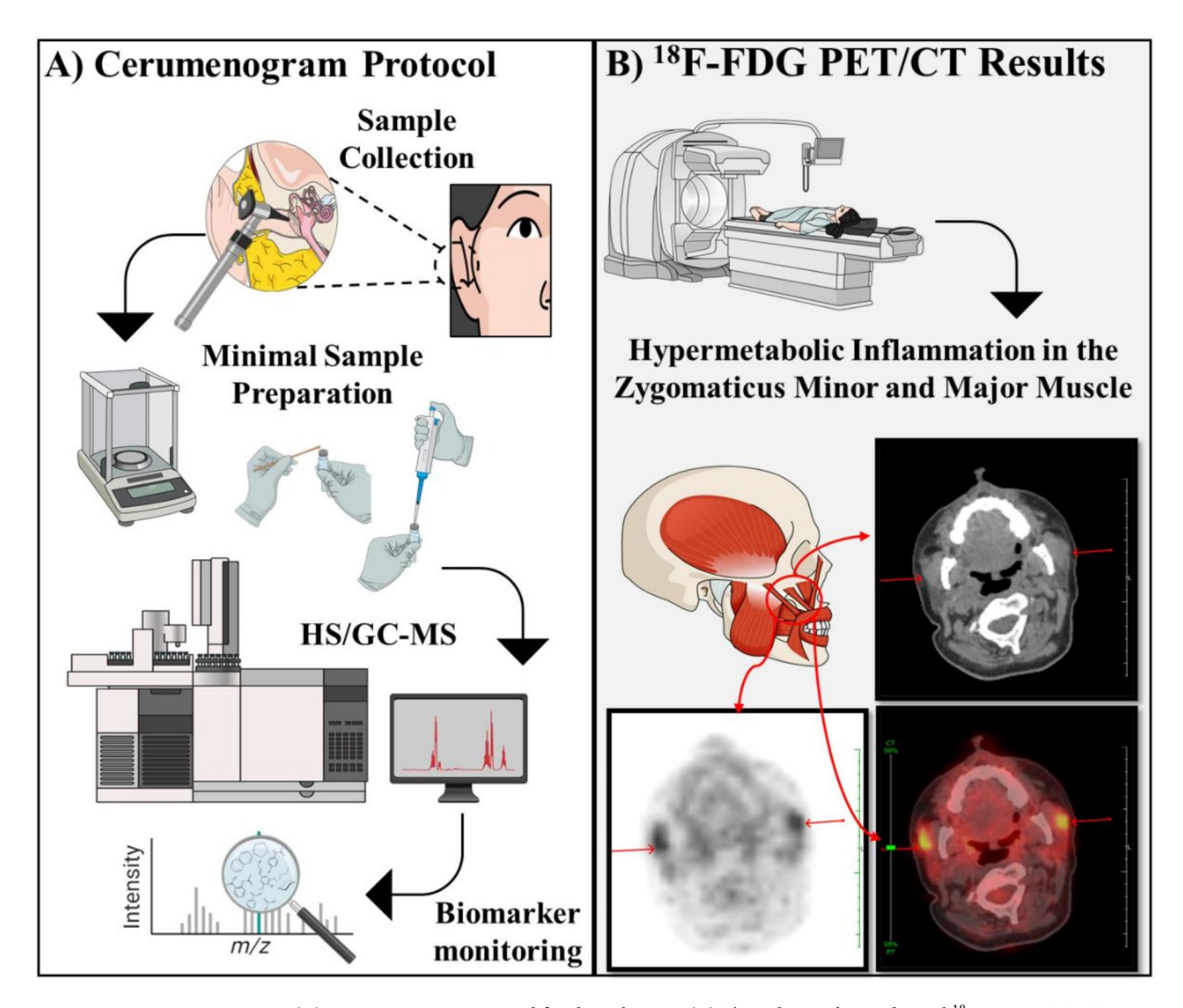


Fig. 2. (A) Cerumenogram protocol for the volunteer. (B) The volunteer's oncological 18 F-FDG PET/CT exam indicated a hypermetabolic region in the zygomaticus minor and major muscles with an SUVmax of 6.9 g mL $^{-1}$.

Investigation of potential precancerous stages using the cerumenogram

Guided by the above-mentioned results regarding using a cerumenogram for successful hypermetabolic inflammation detection, the following steps of this work were to study patients with a confirmed diagnosis of cell abnormalities that may be associated with precancerous stages. Seventeen volunteers who met the diagnostic criteria for metaplasia (n=3), dysplasia (n=3), or benign tumors or cysts (n=11) were enrolled. These seventeen samples (n=17) were added to the cerumenogram database as blind samples (neither labeled the control nor the cancer group).

The samples from the metaplasia group were obtained from volunteers with Barrett's esophagus and gastric intestinal metaplasia. In the dysplasia group, all the volunteers were diagnosed with mammary dysplasia. Volunteers with benign tumors or cysts included patients with benign thyroid nodules, desmoid tumors, renal cortical nodules, benign liver tumors, angiolipomas, retinocytomas, and ovarian and pancreatic cysts.

In evaluating the 17 samples, the Cerumenogram-based model predicted the following samples as part of the oncological risk-free group: all three samples from the metaplasia group and all 11 from benign tumors or cysts. Figures \$13-\$14 present examples of the cerumenogram dendrogram classifying one sample from each group into the oncological risk-free group. In contrast, all samples from the dysplasia group were predicted to belong to the oncological risk group. Figure 3 summarizes the group test, predicted class for each sample, and diagnostic description for each volunteer.

Notably, all samples from patients with dysplasia were predicted to belong to the oncological risk group. Since mammary dysplasia can progress to breast cancer³⁶, the detection of dysplasias can contribute to the prevention and intervention of breast tumorigenesis at the early stages of the disease. Given that the cerumen contains cancer volatile biomarkers potentially resulting from the increased oxidative stress caused by fatty acids

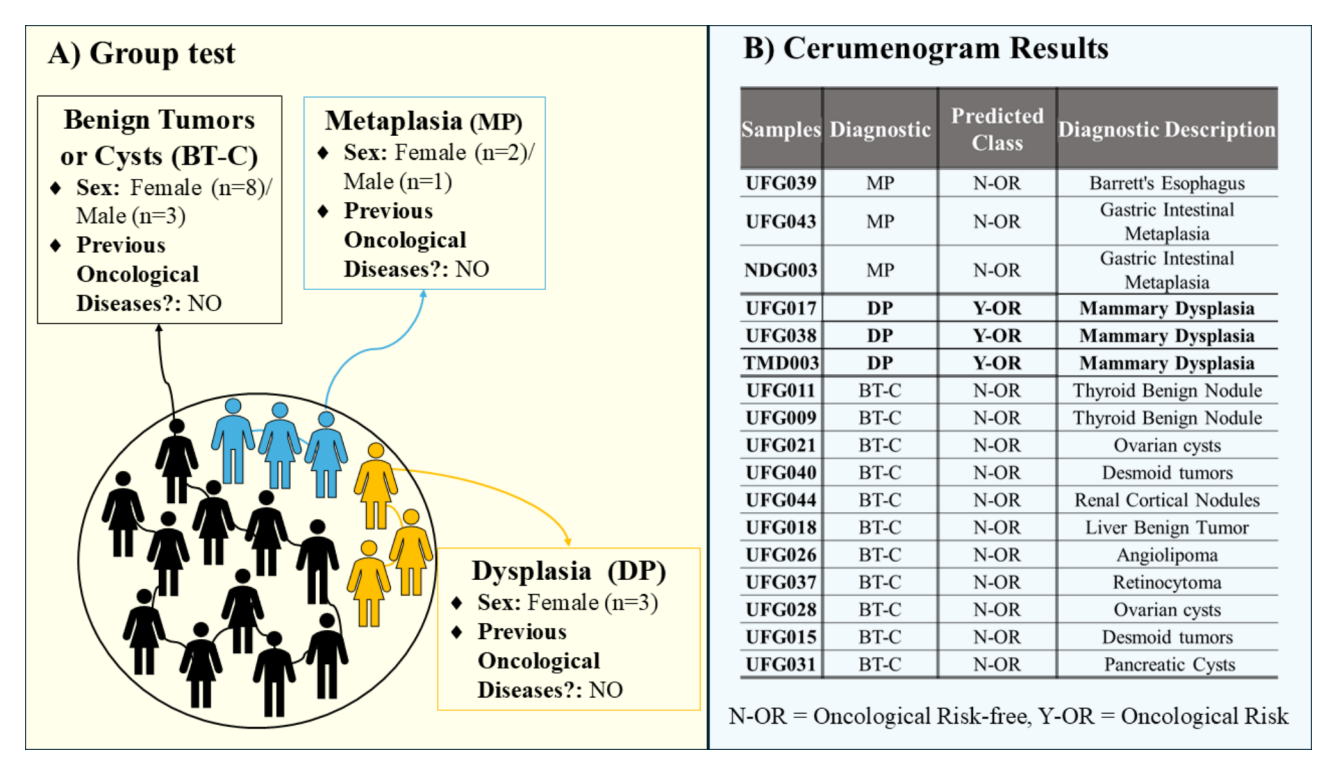


Fig. 3. (**A**) Group test: metaplasia (n = 3), dysplasia (n = 3), and benign tumors (n = 11). (**B**) Sample prediction table showing the sample labels, predicted class by the Cerumenogram assay (N-OR = Oncological Risk-free, Y-OR = Oncological Risk), diagnostic category (MP = Metaplasia, DP = Dysplasia, BT-C = Benign Tumor), and the clinical diagnostic description of each volunteer.

as a consequence of mitochondrial dysfunction in malfunctioning cells^{24,25,37}, the results herein might indicate that the metabolism fingerprint of dysplastic cells suggests that the human body's volatilome is already altered during early carcinogenesis.

However, the same effect was not observed in volunteers with metaplastic cells or those with benign tumors or cysts. The metaplasia process involves replacing a differentiated cell type with another mature differentiated one uncommonly present in a particular tissue due to stress stimulation³⁸. From a volatilomic perspective, the results herein support the findings of Kumar et al. and Amal et al., who detected differential volatile profiles in the breath of patients with malignant manifestations compared to those with metaplasia^{39,40}.

Similarly, the group of volunteers with benign tumors or cysts was not classified in the oncological risk group by the cerumenogram assay. Benign tumors are characterized by a slow growth rate and an inability to spread and invade other parts of the body⁴¹. Cyst manifestations are fluid-filled sacs that develop on different types of organs, and numerous causes can be associated with their origins, such as infections, cell defects, and local inflammation with a considerably low risk of malignancy. The finding that the volunteers with these benign manifestations were classified as part of the oncological risk-free group might indicate that metabolic reprogramming in these cells will likely differ from that in high-risk precancerous lesions such as dysplastic cells.

The correct discrimination of low-risk precancerous lesions from high-risk lesions is crucial because a large number of patients undergo unnecessary invasive procedures to rule out cancer detected using conventional approaches that are suboptimal for distinguishing between malignant and benign nodules⁴². We recognize that the limited availability of precancerous samples in this study may be a limitation, thus necessitating careful interpretation to avoid extrapolating the results. To mitigate this limitation, all samples were analyzed in a blind, randomized manner alongside quality control samples. The cerumenogram assays aligned with earlier studies on precancerous conditions, identifying distinct volatile profiles in patients with malignant conditions compared to those with metaplasia^{39,40}. These results underscore the cerumenogram potential as a decision-making tool for differentiating lesions associated with higher oncological risk from those with lower risk. This study revealed that the volatilomic profile of normal cells shifts to an inflammatory stage during tumorigenesis, advancing to dysplasia and ultimately reaching the neoplasia stage, as shown in Fig. 4.

Detection of cancer recurrence until remission using the cerumenogram

In this case study, the volunteer was a 75-year-old white Brazilian male with a body mass index of 24 kg m^{-2} and a prostate cancer remission diagnosis (more than five years) in his medical history. During a round of sample collection, the volunteer was assigned to the control group (oncological risk-free). Although the volunteers were self-declared as part of the control group, the cerumenogram indicated that the sample was part of the case group (oncological risk). After communicating the outcome, the volunteer agreed to undergo follow-up $^{68}\text{Ga-PET/CT}$ with Protaste-Specific Membrane Antigen (PSMA) fusion imaging (Fig. 5).

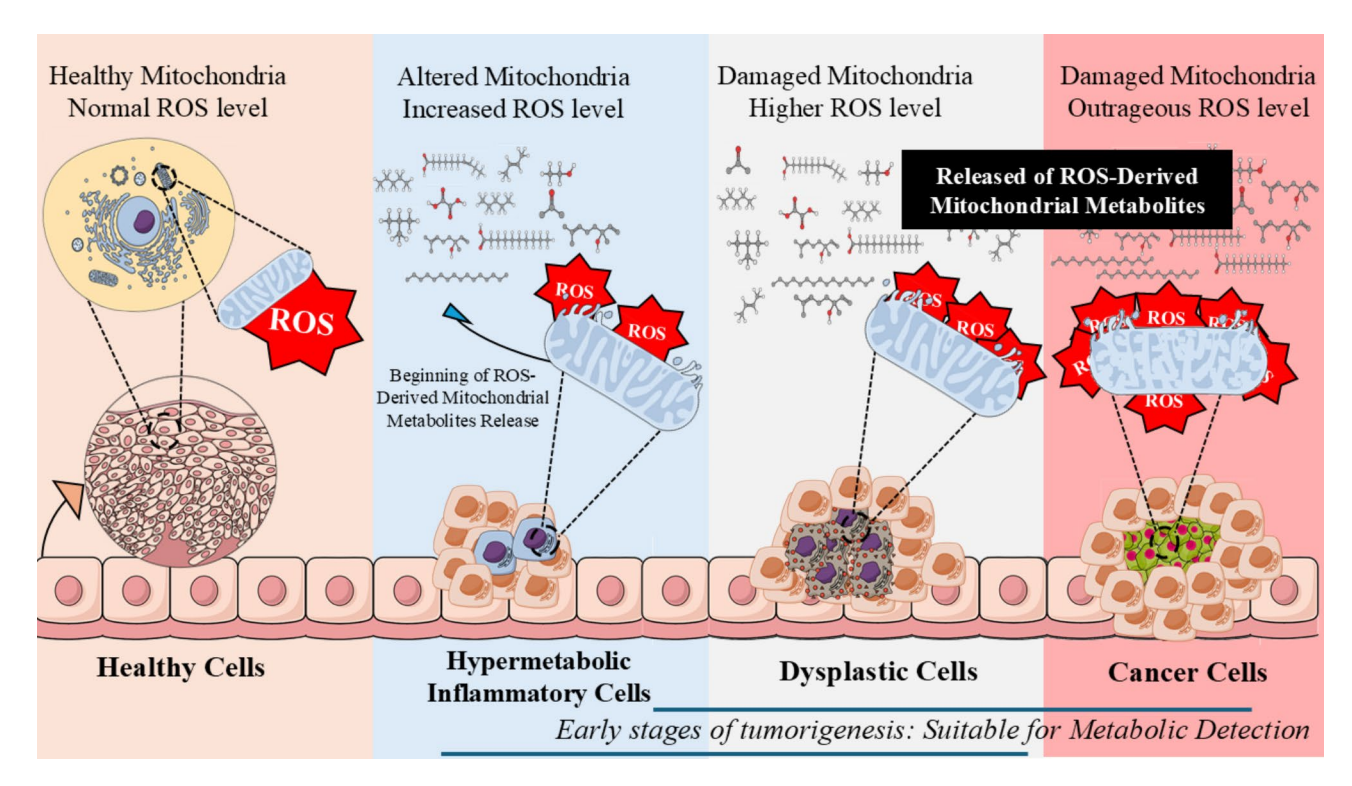


Fig. 4. Tumorigenesis from a volatilomic point of view.

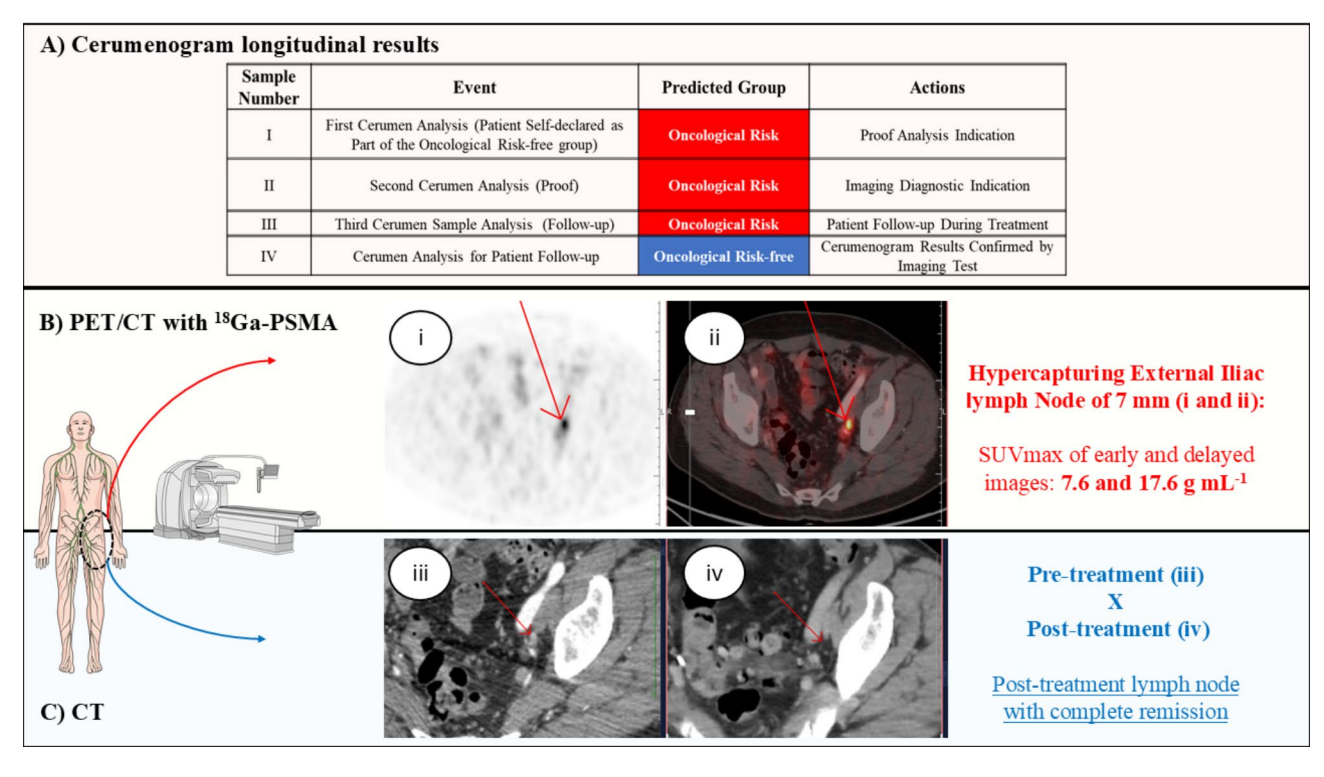


Fig. 5. (**A**) Cerumenogram longitudinal results for the volunteer. Three Cerumenogram analyses classified the sample as part of the oncological risk group; in the fourth analysis, the sample was classified as part of the oncological risk-free group. (**B**) ⁶⁸Ga-PET-CT/PSMA confirmed a hypercapturing lymph node abnormality in the left external iliac lymph node, with SUVmax values of 7.6 and 17.6 g mL⁻¹ in the early and delayed images, respectively. (**C**) Computed tomography (CT) images (iii) before and (iv) after treatment, showing complete remission of the lymph node.

Interestingly, although recent biochemical conventional examinations indicated that the volunteer was in remission with cancer, the ⁶⁸Ga-PSMA-PET/CT results agreed with the findings of the cerumenogram, which indicated a hypermetabolic region in the volunteer characterized by a radiopharmaceutical uptake abnormality in the left external iliac lymph node, indicating a lesion of 7 mm (the SUVmax of early and delayed images was 7.6 and 17.6, respectively). ⁶⁸Ga-PSMA PET/CT results confirmed the presence of neoplastic activity in volunteers. At the request of the oncologist, the patient was subjected to radiotherapy treatment for nine months.

Longitudinal earwax samples were collected from volunteers during cancer treatment by radiotherapy. After treatment, cerumenogram analysis indicated that the volunteer was part of the oncological risk-free group (Fig. 5). The patient underwent imaging examinations, which also revealed remission of neoplastic activity, confirming the positive effect of the treatment. The results indicate that cerumenogram has the potential to become the initial option to assess whether there is a need to carry out costly and hardly accessible tests, such as PET/CT, CT, and MRI, to diagnose the occurrence of hypermetabolic cellular events correlated with oncological risk, as well as to evaluate the cancer treatment progress.

Discussion

This study demonstrated exciting potential applications of cerumenogram in situations that have not been explored before. The fact that hypermetabolic inflammation led to positive oncological risk indications in the cerumenogram may support compelling hypotheses about the chemical environment associated with cancer development. The idea of crosstalk between inflammation and tumorigenesis was first proposed in the mid-nineteenth century, based on the observations of Rudolf Virchow that cancer originated at sites of high inflammatory activity, as confirmed by the abundance of inflammatory cells in tumor biopsies⁴³. Since then, inflammation has been associated with stages of tumorigenesis and malignant progression to metastasis³³. Furthermore, mitochondrial DNA (mtDNA) mutations can promote inflammation during the early stages of tumorigenesis⁴⁴.

Based on the results presented herein, the cellular tumorigenesis process might be associated with the mitochondrial biochemical environment in addition to the genetic alterations in the cell nucleus that block oncosuppressors (such as p53). This observation can be highlighted by detecting metabolic alterations in stages before cancer using the cerumenogram assay by tracking derived mitochondrial metabolites (volatile biomarkers), similar to metabolic dysfunctions noted within neoplastic cells. Thus, a biochemical tool, such as liquid biopsy, could also be used to diagnose early-stage cell cancer; however, the cerumenogram assay can also be used to detect hypermetabolic inflammation and dysplasia, with the advantage of being noninvasive and less expensive.

Interestingly, endogenous VOM production and modulation due to oxidative stress are strongly related to inflammation, resulting in an interconnection between oxidative stress, inflammation, and the unbalanced release of volatile metabolites in humans^{35,37}. VOM production and modulation are well understood as consequences of aberrant oxidative stress, such as increased lipid peroxidation, which is primarily associated with dysfunction in mitochondrial electron transport chain¹¹. Oxidative stress can lead to mitochondrial DNA damage in addition to inducing nuclear DNA double-strand breaks and repair errors, resulting in genomic instability¹¹, one of the hallmarks of cancer⁶.

As cerumen appears to be a suitable biofluid that can concentrate tumor-derived metabolites and is easily accessible in a noninvasive manner, we hypothesized that the cerumenogram could serve as a tool for detecting the early inflammatory processes that may induce cancer growth and progression, as demonstrated in the two case studies presented in this work. Further studies involving individuals with chronic inflammatory diseases and hypermetabolic manifestations will help elucidate the accuracy of cerumenogram detection of these metabolic activities and establish a screening tool for oncological risk as its first manifestation (inflammation associated with tumorigenesis).

However, we evaluated the response to the cerumenogram in an exploratory manner for volunteers who self-identified in the oncological risk-free group but, at the time of cerumen sampling, had tonsillitis and pharyngitis, leading to a negative result on the cerumenogram. This suggests that these types of bacterial inflammation do not exhibit the same tumorigenesis metabolism, particularly hypermetabolic inflammation.

Interestingly, patients with metaplasia and benign tumors or cysts were classified into the oncological risk-free group (Fig. 3). These findings might indicate that the process of abnormal cell growth (benign tumors and cyst manifestations) and the process of replacing one differentiated cell type with another uncommon type in a specific tissue (metaplasia process) are not followed by a substantial increase in oxidative stress activities that can lead to dysregulation of mitochondrial lipid metabolism and genome instability, similar to a cancer initiation process. Another hypothesis is that if volatile metabolites are altered in such situations, they are not the same as those monitored in the cerumenogram biomarker panel²⁴.

Similarly, other studies exploring the volatilome in other biomatrices have also demonstrated a different pattern when comparing the volatile fingerprint of a cancer group and a metaplasia group^{39,40}, which might indicate that there is a crucial metabolic difference in terms of oxidative stress that discriminates between the metaplasia process and the other steps of tumorigenesis.

In contrast, the oncological risk group included samples from patients with mammary dysplasia (Fig. 3). The possible association between benign mammary dysplasia and breast cancer has been discussed since the late 1970s when prospective studies confirmed a higher incidence of breast cancer in patients with biopsy-proven mammary dysplasia than in those without dysplastic manifestations⁴⁵. Mammographic dysplasia is strongly linked to breast carcinogenesis, and detecting the dysplastic process before cancer onset may offer opportunities for early intervention as a preventive strategy.

Notably, a broad range of abnormalities in mitochondrial bioenergetic dysfunction have been observed in various dysplastic cell phenotypes⁴⁶, which might indicate an analogous modulation of volatile metabolites

observed during hypermetabolic inflammation and cancer. The ability of the cerumenogram to detect this precancerous manifestation of breast cancer presents an excellent opportunity for future screening programs, using a noninvasive and affordable early detection method to reduce the number of projected breast cancer deaths—more than one million of which are estimated to occur worldwide by 2040⁴⁷.

The detection of cancer recurrence in an asymptomatic patient and its follow-up during treatment (Fig. 5) might represent another exciting application of the cerumenogram method for measuring treatment effectiveness. The lack of specificity of conventional chemotherapeutic agents and untargeted radiotherapy might be the cause that cancer treatment may not respond effectively to a particular patient⁴⁸. Thus, it is critical to develop a tool for monitoring the effectiveness of cancer treatment and to correlate the results with clinical data to guide decision-making and optimize outcomes.

Conclusion

This work presents the cerumenogram as a suitable tool for (i) detecting oncological risk by identifying premalignant cells before the onset of cancer, which introduces new implications for using this approach as a trial tool for tumor prevention; (ii) finding that mitochondrial impairment in premalignant cells (e.g., hypermetabolic inflammation, dysplasia) produces the same volatile biomarkers for cancer detection, which differ from those in metaplasia and benign tumors, opening new possibilities for patient risk management and early intervention in treating premalignant lesions; (iii) linking the cerumenogram with conventional and well-established diagnostic techniques, such as 2-deoxy-2-[fluorine-18]fluoro-D-glucose integrated with computed tomography (¹⁸F-FDG PET/CT) and ⁶⁸Ga-PET/CT with Protaste-Specific Membrane Antigen (PSMA) fusion imaging, demonstrating that the cerumenogram results align with those obtained from commonly used clinical techniques, offering the advantages of being non-invasive and considerably lower in cost; iv) monitoring cancer treatment and remission, demonstrating a potential application of cerumenogram in assessing the effectiveness of tumor treatment and identifying the transition of cells to a normal state; v) attesting malignance metabolic conditions for clinical decision-making associated with imaging and biopsy tests; vi) generating insights that pave the way for developing new drugs targeting metabolites with increased production in malignant manifestations.

In conclusion, the results presented suggest that the cerumenogram could serve as a valuable assay for assessing precancerous signs, cancer development, and remission. This advancement may play a critical role in reducing mortality, alleviating suffering, and minimizing costs related to the disease.

Materials and methods Ethical approval and volunteers

All volunteers in this study signed a written informed consent form to confirm that they agreed to participate in the "Cerumen Project," which was coordinated by Prof. Dr. Nelson Roberto Antoniosi Filho and approved by the Universidade Federal de Goiás and Hospital Amaral Carvalho ethics committees for research involving humans (Protocol: #57880516.9.0000.5083 and #57880516.9.3003.5434). All the procedures applied in this study strictly followed the principles of the Declaration of Helsinki. The criteria used to select volunteers included: (i) a referral from a physician involved in the project, (ii) submission of an updated medical history confirming their condition and any other comorbidities, (iii) a recent clinical screening to verify their condition through biochemical and/or imaging tests, and (iv) the exclusion of volunteers with metabolic diseases not yet evaluated by the cerumenogram, such as neurological disorders.

Cerumen sample collection

All volunteers involved in this study were selected from the Cerumen Project in Phase II, which included 531 volunteers with proven diagnoses of cancer, 203 volunteers without a prior diagnosis of cancer, 03 volunteers with metaplasia, 03 with dysplasia, and 11 with benign tumors or cysts. This study involved the collection of samples from 751 volunteers.

Cancer samples were obtained from a partnership between Hospital Amaral Carvalho, Jaú, SP, Brazil, and Universidade Federal de Goiás, Goiânia, GO, Brazil. The primary cancer locations and staging ranges for the 531 patients are presented in Table 1. In exploring the impact of patients with metaplasia, dysplasia, and benign tumors or cyst on the cerumenogram model, all volunteers had an up-to-date diagnosis confirmed by tissue biopsy (anatomopathological examination) and imaging techniques, ensuring their condition fits the study's criteria. Supplementary Table 1 (Table S1) summarizes the demographic characteristics (sex, age, body-mass index, ethnicity/race, and lifestyle) of the participants analyzed as confounding variables in the cerumenogram model²⁴.

All selected volunteers were instructed not to perform ear cleaning procedures or use products in and around their ears for 15 days prior to the sample collection round. On the day of sample collection, otolaryngologists clinically evaluated the volunteers to ensure the absence of acute otitis media manifestations, and those meeting the inclusion criteria were selected. Volunteers with acute otitis media manifestations or insufficient earwax production were excluded from the study.

Earwax samples were collected using sterilized metallic curettes (Jobson-Horne probes) via direct application to the horizontal portion of the auditory canal, avoiding any contact with outer parts of the meatus. The collected samples were transferred to sterilized plastic tubes (PCR Clean Eppendorf*) and stored at -20 °C in a freezer for further HS/GC-MS analysis.

HS/GC-MS analysis

The volatile signatures of each volunteer were determined using an untargeted metabolomic approach. Then, 10 mg of each collected earwax sample was precisely weighed in 20 mL HS-GC vials, followed by the addition

of 0.1 μ L of 3-methylcyclohexanone (Sigma-Aldrich, Santa Louis, MO, USA) as the internal standard (IS). Similarly, quality control (QC) blanks spiked with IS were prepared and set across batches to monitor signal and retention time drift. All vials were sealed using gas-tight polytetrafluoroethylene-lined rubber septum magnetic caps, randomized in batches, and sent for HS/GC–MS analysis.

Volatile earwax metabolites were extracted using a Shimadzu AOC-6000 HS autosampler (Shimadzu, Kyoto, Japan) equipped with a 2500 μ L gas-tight syringe, VT60-20 tray, and preheating module (LHS0 Combi Pal) with heating time and temperature control (PAL System, Zwingen, Switzerland). The HS parameters were set at 160 °C (incubation temperature), 60 min (incubation time), 500 rpm (agitation speed), 5 s (agitator on time), 2 s (agitator off time), 5 s (prepurge time), 30 s (postpurge time), 150 °C (syringe temperature), 2500 μ L (injection volume), and 100 mL min⁻¹ (injection flow rate).

The GC system used was Shimadzu Nexis GC-2030 (Shimadzu, Kyoto, Japan). Chromatographic separation was carried out in an analytical capillary column NST-100 ms ($25~\text{m}\times0.25~\text{mm}$ i.d. $\times0.3~\mu\text{m}$ film thickness) with a polyethylene glycol-based stationary phase (NST-Nano Separation Technologies, São Paulo, Brazil) using highpurity helium (99.999%—5.0, White Martins, Goiânia, Brazil) as the carrier gas, with a constant flow of 1.36~mL min⁻¹ and a linear velocity of $45.8~\text{cm s}^{-1}$. The oven program followed the cerumen analysis chromatography protocol²², starting at 30 °C for 5 min, increasing to 45 °C (rate: 2 °C min⁻¹; hold time: 5 min), followed by an increase to 50 °C (rate: 2 °C min⁻¹; hold time: 5 min), increasing to 200~°C (rate: 6 °C min⁻¹), ending with a rise to 250~°C (rate: 5~°C min⁻¹; hold time: 10~min), corresponding to 98.33~min a GC run time.

The MS spectrometer used for the GC system was a Shimadzu QP2020 NX (Shimadzu, Kyoto, Japan). The MS instrument was operated at an ion source temperature of 280 °C, a scan speed of 1666 u s⁻¹, a scan time of 0.3 s, and an electron ionization (EI) mode fixed at 70 eV. Cerumen volatile annotations were confirmed by comparing their MS patterns with the NIST17s mass spectral libraries (National Institute of Standards and Technology, Gaithersburg, MD, USA). Compounds with the same base peak (m/z) and at least 80% similarity with NIST17s library standards were selected as annotated metabolites, which were further confirmed by their relative retention time to the IS in the data alignment step.

Data processing and statistical analysis

HS/GC-MS data were acquired and processed using LabSolutions GCMSsolution Software version 4.50 SP1 (Shimadzu, Kyoto, Japan). All peaks with a peak area > 0 and area/height ratio (A/H) > 3 were annotated as "1." In contrast, a peak area = 0 or with a peak area > 0 but with an A/H < 3 was annotated as a hit "0" in the data matrix. Then, the binary inputs extracted from each sample analysis were added to the cerumenogram database for blind analysis (non-labeled) by tracking the metabolites with higher frequencies in the cerumenogram model²⁴. The statistical analyses, model evaluation, and data visualization were performed using R version 4.1.2 in an RStudio environment (RRID:SCR_000432) and a web-based platform for comprehensive metabolomics data analysis "MetaboAnalyst 5.0 (RRID:SCR_015539, www.metaboanalyst.ca/)" 49 .

Data availability

All data needed to interpret the conclusions are presented in the paper and/or Supplementary Information. Additional raw data related to this study are available upon request from the corresponding authors.

Received: 18 December 2024; Accepted: 4 April 2025

Published online: 22 April 2025

References

- 1. David, A. R. & Zimmerman, M. R. Cancer: an old disease, a new disease or something in between?. *Nat. Rev. Cancer* 10, 728–733 (2010).
- Office for National Statistics. Cancer survival in England: adult, stage at diagnosis and childhood—Patients followed up to 2018. Off. Natl. Stat. 1–37 (2019).
- 3. Crosby, D. et al. Early detection of cancer. Science (80-.) 375, eaay9040 (2023).
- 4. de Martel, C., Georges, D., Bray, F., Ferlay, J. & Clifford, G. M. Global burden of cancer attributable to infections in 2018: A worldwide incidence analysis. *Lancet Glob. Heal.* 8, e180–e190 (2020).
- 5. Organization, W. H. Assessing national capacity for the prevention and control of noncommunicable diseases: report of the 2021 global survey (2023).
- 6. Hanahan, D. Hallmarks of cancer: New dimensions. *Cancer Discov.* **12**, 31–46 (2022).
- 7. Stangis, M. M. et al. The Hallmarks of precancer. Cancer Discov. 14, 683-689 (2024).
- 8. Lopez, J. & Tait, S. W. G. Mitochondrial apoptosis: Killing cancer using the enemy within. Br. J. Cancer 112, 957-962 (2015).
- Chang, J. et al. Genomic alterations driving precancerous to cancerous lesions in esophageal cancer development. Cancer Cell 41, 2038–2050 (2023).
- 10. Wood, H. M. et al. The genomic road to invasion—Examining the similarities and differences in the genomes of associated oral pre-cancer and cancer samples. *Genome Med.* **9**, 53 (2017).
- 11. Sabharwal, S. S. & Schumacker, P. T. Mitochondrial ROS in cancer: initiators, amplifiers or an Achilles' heel?. *Nat. Rev. Cancer* 14, 709–721 (2014).
- 12. Phelan, J. J. et al. Differential expression of mitochondrial energy metabolism profiles across the metaplasia–dysplasia–adenocarcinoma disease sequence in Barrett's oesophagus. *Cancer Lett.* **354**, 122–131 (2014).
- 13. Broza, Y. Y., Mochalski, P., Ruzsanyi, V., Amann, A. & Haick, H. Hybrid volatolomics and disease detection. *Angew. Chemie Int. Ed.* 54, 11036–11048 (2015).
- Barbosa, J. M. G. & Filho, N. R. A. The human volatilome meets cancer diagnostics: Past, present, and future of noninvasive applications. *Metabolomics* 20, 113 (2024).
- 15. Coon, A. M., Dane, A. J., Setzen, G., Cody, R. B. & Musah, R. A. Two-dimensional gas chromatographic and mass spectrometric characterization of lipid-rich biological matrices—Application to human cerumen (Earwax). ACS Omega 7, 230–239 (2022).
- Shokry, E. et al. Earwax metabolomics: An innovative pilot metabolic profiling study for assessing metabolic changes in ewes during periparturition period. PLoS ONE 12, 1–22 (2017).

- 17. Barbosa, J. M. G. et al. A cerumenolomic approach to bovine trypanosomosis diagnosis. Metabolomics 18, 42 (2022).
- 18. Barbosa, J. M. G. et al. A veterinary cerumenomic assay for bovine laminitis identification. *Vet. Res. Commun.* https://doi.org/10.1007/s11259-023-10271-2 (2023).
- 19. Barbosa, J. M. G. et al. A volatolomic approach using cerumen as biofluid to diagnose bovine intoxication by Stryphnodendron rotundifolium. *Biomed. Chromatogr.* 34, e4935 (2020).
- Gonçalves Barbosa, J. M. et al. Identification of cattle poisoning by Bifenthrin via earwax analysis by HS/GC-MS. Biomed. Chromatogr. 35, e5017 (2020).
- 21. Shokry, E. et al. Earwax: A clue to discover fluoroacetate intoxication in cattle. Toxicon 137, 54-57 (2017).
- 22. Shokry, E., de Oliveira, A. E., Avelino, M. A. G., de Deus, M. M. & Filho, N. R. A. Earwax: A neglected body secretion or a step ahead in clinical diagnosis? A pilot study. *J. Proteomics* **159**, 92–101 (2017).
- 23. Shokry, E. et al. Earwax: an innovative tool for assessment of tobacco use or exposure. A pilot study in young adults. *Forensic Toxicol.* 35, 389–398 (2017).
- 24. Barbosa, J. M. G. et al. Cerumenogram: A new frontier in cancer diagnosis in humans. Sci. Rep. 9, 11722 (2019).
- 25. Barbosa, J. M. G. et al. Cancer evaluation in dogs using cerumen as a source for volatile biomarker prospection. *Mol. Omi.* 20, 27–36 (2023).
- Seyfried, T. N., Flores, R. E., Poff, A. M. & D'Agostino, D. P. Cancer as a metabolic disease: Implications for novel therapeutics. Carcinogenesis 35, 515–527 (2014).
- Garavaglia, S. & Sharma, A. A smart guide to dummy variables: Four applications and a macro. In Proc. Northeast SAS users Gr. Conf. 43 (1998).
- 28. Elmassry, M. M. & Piechulla, B. Volatilomes of bacterial infections in humans. Front. Neurosci. 14, 1-11 (2020).
- 29. Hofman, M. S. & Hicks, R. J. How we read oncologic FDG PET/CT. Cancer Imaging 16, 35 (2016).
- 30. Heiden, M. G. V., Cantley, L. C. & Thompson, C. B. Understanding the warburg effect: The metabolic requirements of cell proliferation. *Science* (80-.) 324, 1029–1033 (2009).
- 31. Varricchi, G. et al. Eosinophils: The unsung heroes in cancer?. Oncoimmunology 7, e1393134-e1393134 (2017).
- 32. Aloyouny, A. Y. et al. Intramuscular hemangioma in the zygomaticus muscle: A rare case report presentation and diagnosis. *Int. J. Surg. Case Rep.* 74, 42–45 (2020).
- 33. Zhao, H. et al. Inflammation and tumor progression: Signaling pathways and targeted intervention. Signal Transduct. Target. Ther. 6, 263 (2021).
- Longo, V. et al. In vitro profiling of endothelial volatile organic compounds under resting and pro-inflammatory conditions. Metabolomics 15, 132 (2019).
- 35. Tsutsui, K. et al. GC-MS analysis of exhaled gas for fine detection of inflammatory diseases. *Anal. Biochem.* **671**, 115155 (2023).
- 36. Majoor, B. C. J. et al. Increased risk of breast cancer at a young age in women with fibrous dysplasia. *J. Bone Miner. Res.* 33, 84–90 (2018).
- 37. Ratcliffe, N. et al. A mechanistic study and review of volatile products from peroxidation of unsaturated fatty acids: an aid to understanding the origins of volatile organic compounds from the human body. *J. Breath Res.* 14, 034001 (2020).
- 38. Giroux, V. & Rustgi, A. K. Metaplasia: tissue injury adaptation and a precursor to the dysplasia–cancer sequence. *Nat. Rev. Cancer* 17, 594–604 (2017).
- 39. Kumar, S. et al. Mass spectrometric analysis of exhaled breath for the identification of volatile organic compound biomarkers in esophageal and gastric adenocarcinoma. *Ann. Surg.* **262**, 981–990 (2015).
- 40. Amal, H. et al. Detection of precancerous gastric lesions and gastric cancer through exhaled breath. Gut 65, 400-407 (2016).
- 41. Patel, A. Benign vs malignant tumors. JAMA Oncol. 6, 1488 (2020).
- 42. Paez, R. et al. Update on biomarkers for the stratification of indeterminate pulmonary nodules. Chest 164, 1028-1041 (2023).
- 43. Balkwill, F. & Mantovani, A. Inflammation and cancer: Back to Virchow? Lancet (London, England) 357, 539-545 (2001).
- 44. Diakos, C. I., Charles, K. A., McMillan, D. C. & Clarke, S. J. Cancer-related inflammation and treatment effectiveness. *Lancet Oncol.* 15, e493-503 (2014).
- 45. Renwick, S. B. The possible relationship between mammary dysplasia and breast cancer. Aust. N. Z. J. Surg. 46, 341–343 (1976).
- 46. Hazra, S. et al. Mesenchymal stem cell bioenergetics and apoptosis are associated with risk for bronchopulmonary dysplasia in extremely low birth weight infants. Sci. Rep. 12, 17484 (2022).
- 47. Bray, F. et al. Global cancer statistics 2018: GLOBOCAN estimates of incidence and mortality worldwide for 36 cancers in 185 countries. *CA Cancer J. Clin.* **68**, 1–31 (2018).
- 48. Maeda, H. & Khatami, M. Analyses of repeated failures in cancer therapy for solid tumors: Poor tumor-selective drug delivery, low therapeutic efficacy and unsustainable costs. Clin. Transl. Med. 7, 11 (2018).
- Pang, Z. et al. MetaboAnalyst 5.0: Narrowing the gap between raw spectra and functional insights. Nucleic Acids Res. 49, W388–W396 (2021).

Acknowledgements

The authors thank all the volunteers and the institutional team from Hospital Amaral de Carvalho for their collaboration, which made this work feasible.

Author contributions

N.R.A.F. provided the original ideas, funding acquisition, project coordination, conceptualization, visualization, and study design. C.G.O., M.F.G.S., P.M.M.B., and C.M.M. performed earwax sample acquisition and collection. D.M.M.C. performed biochemical examinations. O.C.F. and L.F.M.V. performed imaging tests. J.M.G.B. performed HS/GC-MS analysis. J.M.G.B., A.E.O., and N.R.A.F. conducted software analysis and interpretation. J.M.G.B. and N.R.A.F. prepared the manuscript, performed the formal investigation, data curation, writing, reviewing, and editing of the manuscript. All the authors have read and approved the final manuscript.

Funding

This work was supported by the Coordenação de Aperfeiçoamento de Pessoal de Nível Superior—Brazil (CAPES)—Finance Code 001—for a fellowship to J.M.G.B. (grant number: # 88887.819724/2023-00); and the management of financial resources by the Agência Nacional do Petróleo, Gás Natural e Biocombustíveis (ANP), Fundação de Apoio à Pesquisa (FUNAPE), Fundação Rádio e TV (RTVE) and Universidade Federal de Goiás (UFG).

Declarations

Competing interests

The authors declare no competing interests.

Ethical approval

All volunteers in this work signed a written informed consent form to confirm that they agreed to participate in the "Cerumen Project" which is coordinated by Prof. Dr. Nelson Roberto Antoniosi Filho and approved by the Universidade Federal de Goiás and Hospital Amaral Carvalho ethics committees for research involving humans (Protocol: #57880516.9.0000.5083 and #57880516.9.3003.5434). All the procedures applied in this study strictly followed the principles of the Declaration of Helsinki.

Additional information

Supplementary Information The online version contains supplementary material available at https://doi.org/10.1038/s41598-025-97440-2.

Correspondence and requests for materials should be addressed to N.R.A.F.

Reprints and permissions information is available at www.nature.com/reprints.

Publisher's note Springer Nature remains neutral with regard to jurisdictional claims in published maps and institutional affiliations.

Open Access This article is licensed under a Creative Commons Attribution-NonCommercial-NoDerivatives 4.0 International License, which permits any non-commercial use, sharing, distribution and reproduction in any medium or format, as long as you give appropriate credit to the original author(s) and the source, provide a link to the Creative Commons licence, and indicate if you modified the licensed material. You do not have permission under this licence to share adapted material derived from this article or parts of it. The images or other third party material in this article are included in the article's Creative Commons licence, unless indicated otherwise in a credit line to the material. If material is not included in the article's Creative Commons licence and your intended use is not permitted by statutory regulation or exceeds the permitted use, you will need to obtain permission directly from the copyright holder. To view a copy of this licence, visit http://creativecommons.org/licenses/by-nc-nd/4.0/.

© The Author(s) 2025